PPPL-CFP--2770

DE93 004078

TITLE OF SYMPOSIUM:

Second Symposium on Cyclic Deformation, Fracture, and Nondestructive Evaluation of Advanced Materials

AUTHORS' NAMES:

Holt A. Murray[1], Irving J. Zatz[1] and John O. Ratka[2]

TITLE OF PAPER:

Fracture Testing and Performance of Beryllium Copper Alloy C 17510

AUTHORS' AFFILIATIONS:

[1] Engineering and Scientific Staff, Princeton University, Plasma Physics Laboratory, P.O. Box 451, Princeton, N.J. 08543

[2] Research and Development Staff Metallurgist, Brush Wellman Inc., Cleveland, Ohio 44110.

Conf-9211134--1

ABSTRACT:

When a literature search and discussion with manufacturers revealed that there was virtually no existing data related to the fracture properties and behavior of any copper beryllium alloy C 17510, a series of test programs was undertaken to ascertain this information for several variations in material process and chemistry. These variations in C 17510 were primarily optimized for combinations of strength and conductivity. While originally intended for use as cyclically loaded high-field, high-strength conductors in fusion energy research, material testing of C 17510 has indicated that it is an attractive and economical alternative for a host of other structural, mechanical and electrical applications.

ASTM tests performed on three variations of C 17510 alloys included both J-integral and plane strain fracture toughness testing (E813, E399) and fatigue crack growth rate tests (E647), as well as verifying tensile, hardness, Charpy, and other well defined mechanical properties. Fracture testing was performed at both room and liquid nitrogen temperatures, which bound the thermal environment anticipated for the fusion components being designed. Fatigue crack propagation stress ratios ranged from nominal zero to minus one at each temperature. In order to confirm the test results, duplicate and independent test programs were awarded to separate facilities with appropriate test experience, whenever possible.

The primary goal of the test program, to determine and bound the fracture toughness and Paris constants for C 17510, was accomplished. In addition, a wealth of information was accumulated pertaining to crack growth characteristics, effects of directionality and potential testing pitfalls. The paper discusses the test program and its findings in detail.

KEY WORDS:

copper beryllium, fracture toughness, fatigue crack propagation, fractography, conductors, cryogenic testing

Introduction

The copper-beryllium (CuBe) family of alloys has a forty year history, having been established in a wide range of high consequence applications and used extensively for high production count components. In general, this family of material is selected for a specific property, whether it is ultimate strength, fatigue resistance, environmental integrity, elevated temperature strength or thermal conductivity.

In a recent design for a large magnet system, a copper-beryllium alloy was designated as the coil conductor material. The conductor specification combined aggressively engineered structural requirements with the need for high thermal and electrical conductivity. A program was initiated to optimize the mechanical and electrical properties of the candidate alloy while maintaining production process practicality for thick member, 2.8 cm (1.1 inch), significant weight (over two ton) components. A separate program was initiated which led to the development of a welding technique for large structural members, composed of the copper-beryllium alloy.

The following paper briefly describes the requirements for the large magnet design, summarizes the results of the program to simultaneously enhance the mechanical and electrical properties of the selected alloy and reports in detail on the extensive material characterization program.

This paper presents the use of a copper beryllium alloy in the role of a high performance structural material intended for a high consequence application.

The Magnet Design Requirements

The Burning Plasma Experiment (BPX) at Princeton University's Plasma Physics Laboratory (PPPL) is a proposed fusion research device dedicated to the study of a fusion nuclear burn. The device is dominated by a Toroidal Field Coil (TFC) system composed of eighteen coils with 21 turns per coil, producing a 9 Tesla magnetic field at the 2.6 m major radius. The coil current is 308 kA and results in a significant conductor thermal excursion, from an initial 80 °K to slightly above room temperature. The key portion of the research device pulse is a ten second, full parameter, flat top when the experimental nuclear burn occurs. The physical design is driven by two requirements; a full load scenario of 3,000 machine cycles at 9 Tesla and a half load operation of 30,000 machine cycles at 6 Tesla.

The complete TFC system is composed of approximately 1.13×10^6 kg (2.5 million pounds) of copper-beryllium alloy conductor, arranged in a modified Bitter coil configuration with the turns constructed from 2.8 cm (1.1 inch) thick plate. The design is driven by the nose section of the conductor where the copper based alloy is both the structural and the conductive element of the magnet design. This design configuration, limited by a space envelope, requires the coil conductor in the nose region to resist the induced magnetic loads without any external support structure.

Because of the activation potential of BPX and the mechanical complexity of the magnet systems, replacement of a failed conductor component is a significant task. Therefore, an aggressive quality assurance program and significant engineering margin in the design are planned. A series of ASTM procedures to inspect both the copper beryllium material and the welds have been established. These methods include ultrasonic inspection and X-ray examination.

The electromagnetic loading of the of the TFC is illustrated in Figure 1 and summarized below:

- the vertical separating force, restrained by the conductor and case is 85×10^6 N (19×10^6 pounds),

- the overturning force of the uncased inner leg, the coil nose, is 16×10^6 N (3.6×10^6 pounds),
- the overturning force of the cased outer leg is 18×10^6 N (4.1×10^6 pounds),
- the centering force of the uncased inner leg is 258×10^6 N (58×10^6 pounds).

Candidate Conductor Materials

Once the general system parameters were established, an extensive survey of candidate conductor materials including copper based materials was performed. No commercially available material was identified which would immediately meet the design criteria for the conductor. Several of the material properties key to this design, including low temperature characteristics, electrical conductivity, thermal conductivity, fracture toughness and fatigue response were unavailable in the literature. The methods of preliminary evaluation of candidate materials included establishing the 15,000 cycle stress range capability for a range of R factors. The factor R is defined as the ratio of minimum stress divided by the maximum stress. A pure tension fatigue test would be characterized by an R factor of greater than zero. Alternately, a stress range excursion, symmetric around zero, where the compressive range is the same magnitude as the tension would have a R factor of -1. Figure 2 illustrates the relative fatigue performance of several of the candidate coil conductor materials.

The Copper-Beryllium Alloy Family

The copper-beryllium alloy family is dominated by copper, typically 98%, and beryllium. In specific compositions, the beryllium is combined with nickel or cobalt to obtain enhanced properties through heat treatment, a sequence of solution annealing and precipitation hardening.

When the beryllium and nickel content are 1.8-2.0 and 0.2 % by weight, respectively, the commercially available alloy (UNS C 17200) exhibits aged properties as detailed in Table 1.

When the beryllium and nickel/cobalt content are 0.2 -0.7 and 1.4 - 2.2 % by weight, respectively, the commercially available alloy (UNS C 17510) exhibits age hardened properties as detailed in Table 2.

The abbreviated requirement for one option of conductor material is detailed in Table 3.

The full design specification for the conductor material contains significant detail including demonstrated performance margin in full size components, biaxial loading capability, fatigue and fracture integrity, low temperature characteristics to liquid nitrogen and high thermal and electrical conductivity.

Through a deliberate selection of composition, prescription of processing steps and selected heat treatment, a range of properties may be achieved within the general specification of the copper-beryllium alloy. Examples of the classic tradeoff between electrical conductivity and yield strength for precipitation hardenable materials are common. However, there are several processing routes to achieve the same yield/conductivity goal. These alternate processes lead to materials with different fatigue, fracture and impact properties.

The copper-beryllium alloys can be manufactured to a favorable combination of strength and conductivity by control of composition, thermomechanical processing and aging treatment. An alloy's properties can be engineered to the requirements of a specific application, for instance where fatigue strength and conductivity levels are targeted by a design. Production of C 17510 starts with a direct chill

(DC) cast billet followed by a conventional wrought processing and subsequent aging to the required strength or other physical property. The materials examined in this program represent a processing sequence, targeted to simultaneously enhance the strength and conductivity. During the course of the program over one hundred process combinations were investigated to establish the optimum manufacturing sequence and map process parameter sensitivity.

Three large plates have been manufactured for PPPL under the BPX program. Three different specifications were developed and three distinct alloy variants of C 17510 were produced in large plate configurations. The alloy and Brush Wellman's trademark designations for these plates which are used in the following discussions are summarized in Table 4 with the yield strength and electrical conductivity detailed.

Each of the C 17510 alloys, designated as A, B and C, were produced in large plate forms. Alloy A and Alloy B measured 1.9 x 76 x 483 cm (0.75 x 30 x 190 inches) and Alloy C was produced in a plate measuring 2.8 x 127 x 635 cm (1.1 x 50 x 250 inches). Figure 3 illustrates the Alloy C plate next to two TF coils of TFTR, the flagship fusion experimental device for the United States. The process details and specifics of the materials properties are contained in a series of program reports [1-4]. The precision electrical conductivity measurements were performed at the National Institute of Standards and Technology and included measurements from 75°K to 300°K [5].

Further process enhancements have been recently performed to expand the strength and conductivity regime. However, these materials have not yet been characterized beyond the ultimate, yield and electrical conductivity at room temperature [6]. A sampling of these electrical conductivity and yield strength values are contained in Table 5.

The strength of this copper beryllium alloy family is derived from the precipitation of metastable phases. The precipitation sequence begins from solid solution with the nucleation of Guinier-Preston (GP) zones. As age hardening progresses, a series of coherent precipitates, followed by partially coherent precipitates form from the GP zones. Intermetallic particles known as beryllides, containing Be and Ni, are formed during solidification and also during thermal processing. The combined effect of the precipitates and beryllides is to increase the strength of the alloy. The increase in strength during aging is characteristic of a precipitation hardenable alloy where the strength reaches a peak value during the aging cycle and decreases as a result of overaging. Electrical conductivity continues to increase monotonically during aging as the solute atoms are depleted from solid solution, resulting in a uniform and homogeneous precipitate distribution.

C 17510 as a Structural Material

The BPX TF conductor material was required to be a structural member with excellent electrical and thermal conductivity. The physical and conductivity properties of copper-beryllium had to be simultaneously enhanced over commercially available material and key performance characteristics had to be established. The conductor alloy of choice, a form of C 17510, compares favorably with a number of conventional high performance structural materials as detailed with typical physicals in Table 6.

Each BPX TF conductor turn is essentially a 2.75 cm thick plate measuring 3.80 x 6.35 m (150 x 250 inches). Due to manufacturing constraints, each turn had to be formed by joining three 1.27 x 6.35 m (50 x 250 inch) plates. Further, each turn had to be joined to the neighboring turn to produce a structurally and electrically continuous element. The design requirements included a weld joint with a 345 MPa (50 ksi) yield strength integrity. A development program was initiated to establish a welding technique to meet the design goal [7-9]. The physical aspects of this weld, using C 17200 weld filler to

join the modified C 17510 plate, compare favorably with typical values for more common high performance structural welds as summarized in Table 7.

Tensile Properties of the Full Size Plates

The tensile properties of the three full size plates, designated Alloy A, B and C are listed in Table 8. Tensile testing was performed at room temperature and 77 °K in conformance with ASTM E8. In general, the room temperature longitudinal (L) and transverse (T) yield strength, tensile strength and elongation indicate that the plates are isotropic in tension. The elastic modulus shows similar isotropy for plates A and C. Plate B shows a lower modulus as a result of unique thermal processing, designed to produce the strength and electrical conductivity indicated.

The tensile properties are a function of temperature, demonstrating an increase in yield strength, tensile strength and ductility at the reduced test temperature. The strength increase occurs independent of modulus, which remains at a value consistent with the room temperature data.

Microstructure

The microstructures of the plates are shown in Figure 4. The microstructure and the grain size vary between the three plates since similar, but not identical processing procedures were employed. Processing of the plates, including hot and cold rolling, resulted in grain elongation in the rolling direction and compaction in the transverse direction. The average grain size of the plates was measured to be 23.3, 25.1 and 49.8 μm for A, B and C respectively. The strength of the plates, detailed in Table 8, is independent of the grain size. Since the material is precipitation hardened, the volume fraction and the distribution of precipitates, not the grain size, establishes the strength and ductility.

Charpy V-Notch

Charpy V-Notch tests, conducted in accordance with ASTM E23, are listed in Table 9. The 77°K, liquid nitrogen, values show an increase in impact toughness at 77°K as compared with the room temperature data. In addition to these greater toughness values, the fibrous shear fracture percentage increases slightly. These results were expected since the material has a face center cubic structure.

While the tensile results indicated the material to be isotropic, the impact toughness values for plate C show otherwise. The room temperature TL and LT values, 16 and 39 J, respectively, show directionality in the impact toughness. The shear fracture percentage substantiates that the LT orientation is inherently tougher than the TL. In reference to the plate processing, the cracks are less blunted in the longitudinal rolling direction than in the transverse direction. The toughness value in the transverse direction increases at 77°K to 24 J without an increase in fibrous fracture.

Fracture Toughness Testing

Over a period of about a year, four independent test programs [10-13] were initiated in an attempt to establish the fracture related material constants of the three candidate CuBe alloys. These tests were to be performed in strict accordance with ASTM standards and included the following in addition to those mentioned previously (E8, E23):

- Plane-Strain Fracture Toughness Tests (ASTM E399)
- J-Integral Fracture Toughness Tests (ASTM E813)
- Fatigue Crack Growth Rate Tests (ASTM E647)

The first test program was awarded for the testing of alloys A and B. The second test series examined A only. The final two programs, initiated after the results of the first two were completed and studied [14], examined alloy C, only, which was developed, in part, based on the results of the initial tests on alloys A and B.

All fracture toughness tests (E399 and E813) were performed on 19.1 mm (0.75 in.) thick standard compact tension (C(T)) specimens, conforming with the alloy a and B plate thicknesses. The fatigue crack growth rate tests were all performed on center cracked panels (M(T)) measuring 290.5 x 101.6 x 9.5 mm (11.4 x 4.0 x 0.375 in.). M(T) specimens are indicted by the ASTM for testing at stress ratios (R = Smin/Smax) that are less than zero. Since the intended application of the alloy as a conductor was for conditions whose value of R would predominantly be less than zero, only M(T) specimens were tested, including those at nominal zero, for consistency. Tests were performed almost entirely at room and liquid nitrogen temperatures. It was anticipated that all varieties of the C 17510 alloy would probably be too tough for this specimen thickness to produce consistently valid plane strain E399, results, especially at room temperature; therefore, a matrix of E399 and E813 specimens were prepared with the expectation that the J_{IC} results would be the more valid of the two toughness specimens. Since some materials become more brittle (less tough) while strength increases at lower temperatures, it was anticipated that the E399 tests could possibly produce more valid results at liquid nitrogen than at room temperature, with E813 tests again to be performed as backup, if necessary.

With so little known about the fracture properties of C 17510, certain assumptions had to be made prior to testing. For example, based on the geometry of the proposed toroidal field coil, and the fact that the static properties indicated essentially isotropic behavior, the first two sets of toughness specimens (alloys A and B) were cut and the tests conducted on only one orientation of the CuBe plate, the L-T direction, as indicated in Figure 5. The intent was to orient the specimens during the tests so that cracks would propagate in the transverse direction, the more critical, shorter, radial direction of the magnetic coil. Consistent with this, the principal design loads on the coil are in the longitudinal direction.

While the results of every E399 test in the initial programs for alloys A and B were invalid (the materials, not surprisingly, being too tough and ductile for these specimen thicknesses even at liquid nitrogen temperatures) the failure mechanism for every specimen was similar and unexpected. Rather than the specimen cracking normal to the applied load direction and along the prescribed notch, as is usually the case, the cracks turned near 90-degrees and failed parallel to the load direction. This mode II-type shearing failure, unusual for metallic materials, was attributed, in part, to the fact that the CuBe plates were primarily rolled in one direction, longitudinally, which may affect the grain structure of the material in such a way as to render that direction a more preferred crack propagation plane than the transverse direction, the direction normal to the rolling and to the applied load. Therefore, regardless of how a C(T) specimen is oriented, it became clear that the preferred crack path and rupture plane will ultimately be in the longitudinal, or rolled, direction. With this knowledge in hand, when the final two test programs for alloy C were prepared some months later, toughness specimens were cut in both the L-T and T-L orientations, with valid E399 results obtained for the alloy's preferred T-L direction. Figure 6 shows typical failed E399 specimens for all three alloys in the L-T orientation. Figure 7 is a matrix of alloy C specimens that contrast the effects of temperature and orientation.

The E813 fracture toughness tests benefitted from the E399 tests that preceded them. Almost all J_{IC} specimens were side-grooved after the pre-cracking portion of each test (per ASTM guidelines). Side-grooving reduces the area of the desired fracture plane normal to the load direction and attempts to

force the failure in the preferred transverse direction and within acceptable ASTM standards. In the case of CuBe, side-grooving in the E813 tests would help to prevent the crack from making the anticipated near 90-degree turn experienced in the E399 L-T tests, where side-grooving is not permitted per the ASTM. Figure 8 shows the effects of side-grooving for the L-T orientation of alloy A. As with the E399 tests, the E813 tests on alloys A and B were all of the L-T orientation and alloy C tests examined both L-T and T-L. Several of the J_{IC} specimens, including side-grooved L-T's, produced valid results with others coming extremely close to the meeting the ASTM criteria. Figure 9 shows typical failed E813 specimens for all three alloys in the L-T orientation. Figure 10 is a matrix of alloy C specimens that contrast the effects of temperature and orientation.

Based on the limited number of valid J_{IC} and K_{IC} tests, the values of fracture toughness for the three C 17510 alloys cannot be determined with certainty, but Table 10, which summarizes the toughness testing results, can be used to estimate values of fracture toughness that can be used for comparison with other materials and for life prediction calculations.

Fractography

Representative plane strain fracture toughness (K_{IC}) compact tension specimens, tested at room temperature and 77°K, were selected for scanning electron microscopy (SEM) examination of the fracture surface. The unusual fractures seen in Figure 6, were typical of specimens in the LT orientation. In contrast, specimens tested in the TL orientation developed a more conventional planar appearance.

In Figure 11, the fracture surfaces are shown from plate C which was tested, oriented in the TL direction, at room temperature and 77°K. These specimens exhibit ductile rupture with a mix of conical and shallow dimples. The fracture mode is primarily transgranular with some intergranular character. Small particles, intermetallic beryllides, are seen within several of the dimples. The specimen tested at 77°K displays a greater degree of tearing and a variety of dimple sizes.

Plate C, tested in the LT orientation displays secondary cracking. These secondary crack paths, shown in Figure 12, are intergranular and were evidenced both at room temperature and 77°K. The extent of ductile tearing and the development of secondary cracks increases at the low test temperature, as illustrated in Figure 12. The fracture character and crack propagation is similar for plates A and B. LT specimens, tested at 77°K are shown in Figures 13 and 14, for A and B, respectively. Each display transgranular ductile fracture with secondary cracking.

Fatigue Crack Growth Rate Testing

Given the limitations of time and money, the fatigue crack growth rate testing could not be totally comprehensive considering the many variables associated with this type of test, but the tests still produced several significant findings that reflect a greater understanding for the behavior of the C 17510 alloy family. As with the toughness tests, the first two test programs performing procedure E647, examined the L-T orientation of alloys A and B, only. While only a limited amount of crack growth testing was performed on alloy B at room temperature and R = -1, a greater amount of testing was performed on alloy A, filling a matrix of conditions at R equals nominal zero and minus one at both room and liquid nitrogen temperatures with multiple specimens for each condition duplicated independently at two different test facilities. Fortunately, the required M(T) specimen for negative stress ratios was ideally suited to test the L-T direction. If the more typical compact-type C(T) specimen had been used, there almost certainly would have been Mode II-type crack propagation paths that turn in the longitudinal direction as

was observed in the toughness tests. But, by virtue of its symmetry in geometry and load, the M(T) specimen was effectively able to study the more desirable Mode I L-T direction crack propagation.

Optical observation of the crack fronts during testing revealed that the crack tip, in actuality, frequently branched in several directions at once resulting in multiple crack tips at each front. This resulted in a somewhat irregular cracking plane as the overall crack progressed and continued branching. From a testing standpoint, this is not an overly desirable behavioral pattern; however, from a practical applications standpoint, the multiple crack fronts is indicative of the materials' ductility and energy absorption capabilities when in service, making it a desirable candidate structural material.

The latter alloy C tests, which studied both the L-T and T-L crack growth orientations, also employed the M(T) specimen exclusively for all tests. In addition to testing multiple specimens in both orientations at both room and liquid nitrogen temperatures for stress ratios of nominal zero and minus one, as with the alloy A tests, alloy C tests were also performed at an intermediate value of R = -0.25 at room temperature for the L-T and T-L directions tying it to a performance condition of the BPX conductor.

The principal goal of the E647 tests was to study Stage II crack growth and thereby determine the Paris constants from the log-log plots of crack growth rate versus stress intensity range for the three alloys at each set of testing conditions. The variation in constants would help to establish the sensitivity of the alloys to stress ratios and temperature. As a result of this fundamental goal, and the aforementioned testing limitations, no attempt was made to study the more complex crack growth approaches such as closure theory or fitting to the Forman equation. Nevertheless, the crack growth tests provided valuable additional data that supplemented the Paris constants. For example, initial crack growth testing was carefully performed at relatively low applied loads and rates in order to ascertain where Stage II growth began. As a result, a rough estimate of Stage I growth and, in turn, an estimate of the threshold stress intensity could be made from the data which consistently indicated a value of approximately 10 MPa$\sqrt{m}$ ($\approx$10 ksi$\sqrt{in}$) for the L-T direction in all three alloys. T-L tests indicated a value of threshold stress intensity that was slightly less than the L-T tests ($\approx$ 8-9 MPa $\sqrt{m}$). Similarly, an examination of the final Stage III data points of crack growth just prior to failure yielded approximate values of fracture toughness that could be compared to the values obtained by the toughness tests. Figure 15 compares the surfaces of alloy C specimens at room temperature in the L-T orientation for three different stress ratios. Figure 16 does the same for T-L orientation specimens. Figure 17 contrasts the surfaces of the three alloys for room temperature, R = -1, L-T orientation conditions. Figure 18 compares crack surfaces of alloy A, L-T orientation, for three different temperatures, all at a stress ratio of minus one.

In general, the E647 tests in all four test programs went extremely well with frequent tight overlaying of data points and Paris constants nearly duplicated consistently for common testing parameters in the various test programs providing additional validity to the results. Typical consistency of test results can be seen in Figures 19 and 20 which depict different conditions for different alloys. Table 11 summarizes the Paris constants from these test programs for all three alloys.

Several fatigue crack growth tests were performed at an intermediate cryogenic temperature of 150°K. This was done to determine the Paris constants at a temperature near to one of the potential operating levels of the designed magnets as well as to study the linearity of the constants as a function of temperature. Unfortunately, technical difficulties during the tests produced sufficient scatter and uncertainty in the data to render the results invalid. The problem, which resulted from the formation of unanticipated ice crystals at the crack tip, was attributed to the presence of excessive moisture in the cryogenic testing chamber which would not be present in a pure liquid nitrogen bath and not be a concern at room temperature. The importance of obtaining additional crack growth data at additional temperatures remains a high priority.

Summary

Based on the material development program described in this paper, copper-beryllium alloy C 17510 shows enormous potential as a structural material that can be utilized in a wide variety of special applications. Originally optimized for use as a low temperature, high strength, high conductivity material in an experimental fusion device, the favorable fracture and fatigue capabilities as well as environmental integrity and excellent welding characteristics of C 17510 suggests its use in many other industrial and commercial situations. The alloy has shown potential to be further engineered depending on the specific needs demanded by particular circumstances. While the work presented herein is by no means comprehensive or totally complete, it represents a first step in what plans to be an ongoing experimental program to further establish C 17510 as a viable candidate material, supported by the favorable findings from these material tests. Future work will propose additional specific applications for copper-beryllium in conjunction with additional testing.

Acknowledgements and Notes

This work was performed, in part, under U.S. DOE contract DE-AC02-76CH03073.

Note that copper-beryllium, like many industrial materials, poses a health risk only if mishandled. In its usual solid form, as well as for finished parts, and in most manufacturing operations, it is completely safe. However, breathing very fine particles may cause a serious lung condition in a small percentage of individuals. Risk can be minimized with simple, proven, and readily available engineering controls such as ventilation of operations producing fine dust. Information on safe handling procedures is available from Brush Wellman Inc.

References

1. Optimization of Toroidal Field Coil Conductor Properties for BPX, 14th IEEE/NPSS Symposium on Fusion Engineering, IEEE catalog number 91CH3035-3, Robert Ellis III and Holt Murray, Princeton Plasma Physics Laboratory, Post Office Box 451, Princeton, New Jersey, 08544

2. BPX Toroidal Field Coil Design, 14th IEEE/NPSS Symposium on Fusion Engineering, IEEE catalog number 91CH3035-3, P.J. Heitzenroeder, Princeton Plasma Physics Laboratory, Post Office Box 451, Princeton, New Jersey, 08544

3. Characterization of Copper-Beryllium Alloy C 17510, 14th IEEE/NPSS Symposium on Fusion Engineering, IEEE catalog number 91CH3035-3, Holt Murray, Princeton Plasma Physics Laboratory, Post Office Box 451, Princeton, New Jersey 08544

4. Beryllium Copper Plate for the Compact Ignition Tokamak Toroidal Field Coils, Final Report, TR-950, William D. Spiegelberg, Brush Wellman Inc., Cleveland, Ohio, 44110, March,1989.

5. Copper Alloy Resistivity Measurements, National Institute of Standards and Technology (NIST), Report Number 814-32-91, September, 1991, prepared by C. A. Thompson, Electromagnetic Technology Division, Electronics and Electrical Engineering Laboratory, National Institute of Standards and Technology, Boulder, Colorado, 80303

6. Process Parameter Mapping for Alloy C 17510, Final Report, TM-1063, William D. Spiegelberg, John O. Ratka and Edward J. Davidge, Brush Wellman Inc., Cleveland, Ohio, 44110, September,1992

7. Development of a Welding Procedure for High Conductivity Copper-Beryllium Alloy C 17510, 14th IEEE/NPSS Symposium on Fusion Engineering, IEEE catalog number 91CH3035-3, Holt Murray, Princeton Plasma Physics Laboratory, Post Office Box 451, Princeton, New Jersey 08544, Ian D. Harris, Edison Welding Institute, 1100 Kinnear Road, Columbus, Ohio, 43221 and John O. Ratka, Brush Wellman Inc., Cleveland, Ohio, 44110

8. Welding Procedure Development for High Conductivity Beryllium Copper, Edison Welding Institute Report Number J5229, Ian D. Harris, Edison Welding Institute, 1100 Kinnear Road, Columbus, Ohio, 43221 and John O. Ratka, Brush Wellman Inc., Cleveland, Ohio, 44110

9. Gas Metal Arc Welding Procedure Development for Thick Section Beryllium-Copper Plate, Edison Welding Institute Report Number J5491, Ian D. Harris, Edison Welding Institute, 1100 Kinnear Road, Columbus, Ohio, 43221 and John O. Ratka, Brush Wellman Inc., Cleveland, Ohio, 44110, February, 1992.

10. Zatz, I. J. and Murray, H., Final Report of BeCu Material/Crack Propagation Studies Performed by CORRPRO/PSG Engineering, Inc., PPPL EAD-3989, PPPL-F-910614-14, June 14, 1991, Princeton Plasma Physics Laboratory, Post Office Box 451, Princeton, New Jersey 08544

11. Zatz, I. J. and Murray, H., Final Report of BeCu Material/Crack Propagation Studies Performed by Fatigue Technologies, Inc., PPPL EAD-4041, July 31, 1991, Princeton Plasma Physics Laboratory, Post Office Box 451, Princeton, New Jersey 08544

12. Zatz, I. J. and Murray, H., Final Report of BeCu Material/Crack Propagation Studies Performed by CORRPRO/PSG Engineering, Inc., PPPL EAD-4099, November 6, 1991, Princeton Plasma Physics Laboratory, Post Office Box 451, Princeton, New Jersey 08544

13. Zatz, I. J. and Murray, H., Final Report of BeCu Material/Crack Propagation Studies Performed by CORTEST Laboratories, PPPL EAD-4282, August 18, 1992, Princeton Plasma Physics Laboratory, Post Office Box 451, Princeton, New Jersey 08544

14. Fracture Testing of Copper-Beryllium Alloy C 17510, 14th IEEE/NPSS Symposium on Fusion Engineering, IEEE catalog number 91CH3035-3, Irving J. Zatz and Holt Murray, Princeton Plasma Physics Laboratory, Post Office Box 451, Princeton, New Jersey, 08544

Tables

Table 1 - Typical characteristics of commercially available UNS C 17200.

Material Property	Typical Property Values
Yield Strength	1,035 - 1,400 MPa (150 - 200 ksi)
Elongation	5 - 15 %
Fatigue Strength, 10^8 cycles	345 - 414 MPa (50 - 60 ksi)
Electrical Conductivity	15 - 28 % IACS at room temperature

Table 2 - Typical characteristics of commercially available UNS C 17510.

Material Property	Typical Property Values
Yield Strength	345 - 517 MPa (50 - 75 ksi)
Elongation	5 - 20 %
Fatigue Strength, 10^8 cycles	207 - 310 MPa (30 -45 ksi)
Electrical Conductivity	45 -60 % IACS at room temperature

Table 3 - Characteristics of one option of conductor material.

Material Property	Typical Property Values
Yield Strength	724 MPa (105 ksi)
Elongation	15 %
Fatigue Strength	360 MPa (52 ksi) for 3,000 cycles 328 MPa (47.5 ksi) for 30,000 cycles
Electrical Conductivity	68 % IACS at room temperature

Table 4 - Designations and properties for three versions of C 17510.

Alloy	Trademark Designation	Electrical Conductivity	0.2% Yield Strength
Alloy A	Hycon 3HP™58150	58 % IACS	758 MPa (110 ksi)
Alloy B	Hycon 3HP™70080	70	552 (80)
Alloy C	Hycon 3HP™68105	68	724 (105)

Table 5 - Designations and properties for five versions of C 17510.

Designation	Electrical Conductivity	0.2% Yield Strength
Heat 25030/5259-8	77.0 % IACS	565 MPa (82.0 ksi)
Heat 25030/4362-8	74.0	599 (86.9)
Heat 25030/4354-8	74.3	590 (85.6)
Heat 33881/5047-6	70.5	675 (97.9)
Heat 22840/7232-3	63.2	805 (116.9)

Table 6 - Typical physicals for a variety of high performance structural materials.

Material	0.2% offset Yield Strength	Ultimate Strength
C 17510	723 MPa (105 ksi)	792 MPa (115 ksi)
Ti grade 12	413 (60)	517 (75)
Alloy C-4	345 (50)	792 (115)
Alloy 825	310 (45)	689 (100)
316L	172 (25)	482 (70)
304L	172 (25)	482 (70)

Table 7 - Typical physicals for a variety of high performance structural welds.

Weld Material	0.2% offset Yield Strength	Ultimate Strength
C 17510/C 17200	586 MPa (85 ksi)	655 MPa (95 ksi)
Ti grade 12	482 (70)	551 (80)
Alloy C-4	551 (80)	723 (105)
825/NiCrMo	482 (70)	758 (110)
316L	448 (65)	586 (85)
304L	413 (60)	551 (80)

Table 8 - Mechanical and physical properties of CuBe alloy C 17510.

Plate ID	0.2% Yield Strength MPa (ksi)			Ultimate Strength MPa (ksi)			Elongation (% in 1 inch)			Elastic Modulus (10^6 MPa)				Electrical Conductivity (% IACS)	
	RT		77°K	RT		77°K	RT		77°K	RT		77°K		RT	77°K
	L	T	L	L	T	L	L	T	L	L	T	L	T		
A	772 (112)	745 (108)	827 (120)	883 (128)	848 (123)	972 (141)	16	16	20	133 (19.3)	132 (19.2)	134 (19.5)	–	58	118
B	565 (82)	579 (84)	634 (92)	676 (98)	662 (96)	124 (118)	20	20	25	119 (17.3)	–	120 (17.4)	–	70	140
C	724 (105)	703 (102)	745 (108)	800 (116)	752 (109)	827 (120)	14	13	15	134 (19.5)	138 (20 0)	131 (19.0)	128 (18.5)	68	165

Note: Brush Wellman Inc. Alloy Designation: A) Hycon 3HP™58110, B) Hycon 3HP™70080, C) Hycon 3HP™68105

Table 9 - Impact toughness of CuBe alloy C 17510, Charpy V-notch.

Plate ID	Orientation	Room Temperature J (ft - lb)	% Shear	77°K J (ft - lb)	% Shear
A	LT	50 (37)	30	68 (50)	40
B	LT	81 (60)	50	85 (63)	50
C	LT	39 (29)	55	56 (41)	60
C	TL	16 (12)	5	24 (18)	5

Note: Brush Wellman Inc. Alloy Designation: A) Hycon 3HP™58110, B) Hycon 3HP™70080, C) Hycon 3HP™68105

Table 10--Summary of Fracture Toughness Testing (ASTM E399 and E813)

Alloy	Test Condition, Report Reference		K_Q's (MPa√m)	(ksi√in)
A	LT/RT	[10]	102.1, 91.3, 104.3	92.9, 83.1, 94.9
		[11]	81.0, 88.6, 81.3	73.7, 80.6, 74.0
	LT/INT	[11]	91.3, 85.4	83.1, 77.7
	LT/LN	[10]	123.2,129.3,128.4	112.1,117.7,116.9
		[11]	93.0, 91.5	84.6, 83.3
B	LT/LN	[10]	94.6, 101.5, 100.8	86.1, 92.4, 91.7
C	LT/RT	[12]	89.3, 83.2	81.3, 75.7
	LT/LN	[12]	100.0, 109.7	91.0, 99.8
	TL/RT	[12]	63.6, 59.2*	57.9, 53.9*
	TL/LN	[12]	98.6, 95.7	89.7, 87.1

Alloy	Test Condition, Report Reference		J_Q's (kN/m)	(lb/in)
A	LT/RT	[10]	97, 89, 92	554, 508, 526
		[11]	33, 158[a], 37	191, 902[a], 214
	LT/LN	[10]	218, 262, 162	1243, 1494, 927
		[11]	201, 318[a], 171	1148,1814[a], 978
B	LT/RT	[10]	85, 75, 80	488, 428, 454
C	LT/RT	[12]	23, 20, 27	134, 112, 156
		[13]	135, 143, 135	771, 817, 771
	LT/LN	[12]	54, 94, 73	307, 537, 418
		[13]	257, 251*, 258	467,1433*,147
	TL/RT	[12]	26, b, b	151, b, b
		[13]	56, 57, 55	320, 314, 325
	TL/LN	[12]	72, 71, 63	412, 404, 358
		[13]	130*,128*,134*	742*,731*,765

Notes:1. * - This specimen was valid according to all ASTM test criteria 2. a - Indication of a J_{IC} specimen that was not side grooved 3. b - Indication of not enough valid data points for curve fit

Table 11 - Summary of Paris Constants Based on Fatigue Crack Growth Rate Tests (E647)

Alloy	Test Condition	# of specimens/ Report Ref.	C (m/cycle)	C (in/cycle)	n
A	LT/R=0/RT	2 / [10]	8.943E-11	3.521E-09	2.330
		2 / [11]	6.782E-11	2.670E-09	2.460
	LT/R=-1/RT	3 / [10]	4.191E-11	1.650E-09	2.603
		2 / [11]	1.420E-10	5.590E-09	2.270
	LT/R=0/LN	2 / [10]	1.418E-11	5.583E-10	2.812
		2 / [11]	1.515E-11	5.964E-10	2.878
	LT/R=-1/LN	3 / [10]	1.158E-11	4.561E-10	2.895
		2 / [11]	2.131E-11	8.390E-10	2.834
	LT/R=-1/INT	3 / [11]	-----	-------	---*
B	LT/R=-1/RT	2 / [10]	2.929E-11	1.153E-09	2.866
C	LT/R=0/RT	2 / [13]	2.224E-11	8.755E-10	2.728
	LT/R=-1/RT	2 / [13]	3.249E-11	1.279E-09	2.777
		2 / [12]	2.083E-11	8.199E-10	2.879
	LT/R=0/LN	2 / [13]	3.373E-12	1.328E-10	3.055
	LT/R=-1/LN	2 / [13]	5.347E-12	2.105E-10	3.100
		2 / [12]	9.649E-12	3.799E-10	3.020
	LT/R=-0.25/RT	2 / [12]	2.045E-11	8.051E-10	2.801
	TL/R=0/RT	2 / [13]	2.601E-12	1.024E-10	3.662
	TL/R=-1/RT	2 / [13]	6.515E-12	2.565E-10	3.496
		2 / [12]	5.017E-12	1.975E-10	3.536
	TL/R=0/LN	2 / [13]	6.365E-13	2.506E-11	3.660
	TL/R=-1/LN	2 / [13]	2.446E-12	9.629E-11	3.467
		2 / [12]	4.592E-12	1.808E-10	3.322
	TL/R=-0.25/RT	2 / [12]	4.475E-12	1.762E-10	3.510

Notes on determination of constants:

1. Data fit by linear regression analysis
2. The Stage II range was generally set between 2.54E-08 to 2.54E-06 m/cycle (1.0E-06 to 1.0E-04in/cycle) with a few specimens lower bound set at 1.27E-08 m/cycle (5.0E-07 in/cycle)
3. Abbreviations: RT=room temperature; LN=77°K, liquid nitrogen; INT=150°K
4. * - This data was felt to be unreliable due to its scatter

Figure Captions

FIG. 1--The load summary of the BPX TF Coil.

FIG. 2--The stress range vs. R for 15k cycle life.

FIG. 3--The alloy C plate adjacent to the TFTR TF Coils.

FIG. 4--Composite microstructure of C 17510 plates, left to right, alloy A, B and C, at 60x magnification.

FIG. 5--Schematic of CuBe plate orientation with respect to the BPX TF Coil and test specimens.

FIG. 6--Typical plane strain fracture toughness specimens for the three alloys in the LT orientation.

FIG. 7--Alloy C plane strain fracture toughness specimens indicating orientation and temperature.

FIG. 8--The effects of side grooving on J_{IC} alloy A specimens in the LT orientation.

FIG. 9--Typical J_{IC} fracture toughness specimens for the three alloys in the LT orientation.

FIG. 10--Alloy C J_{IC} fracture toughness specimens indicating orientation and temperature.

FIG. 11--SEM micrograph of alloy C plate, TL orientation, tested at room temperature, top, and 77°K.

FIG. 12--SEM micrograph of alloy C plate, LT orientation, tested at room temperature, top, and 77°K.

FIG. 13--SEM micrograph of alloy A plate, LT orientation, tested at 77°K.

FIG. 14--SEM micrograph of alloy B plate, LT orientation, tested at 77°K.

FIG. 15--Comparison of alloy C crack growth surfaces for three different stress ratios-room temperature, LT orientation.

FIG. 16--Comparison of alloy C crack growth surfaces for three different stress ratios-room temperature, TL orientation.

FIG. 17--Comparison of crack growth surfaces for the three alloys-room temperature, LT orientation, R=-1.

FIG. 18--Comparison of alloy A crack growth surfaces at three different temperatures-LT orientation, R=-1.

FIG. 19--da/dN vs. ΔK plot for three specimens-alloy A, room temperature, LT orientation, R=-1.

FIG. 20--da/dN vs. ΔK plot for two specimens-alloy C, LT orientation, 77°K, R=-1.

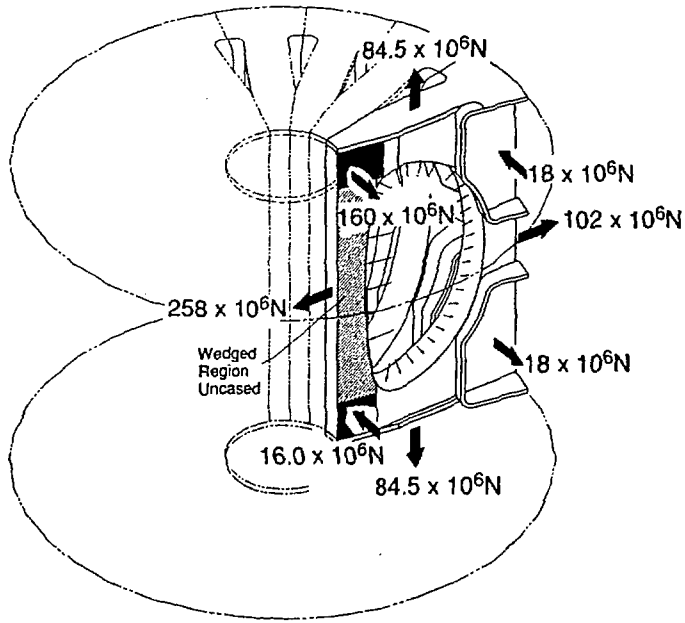

FIG. 1 (ZATZ, MURRAY, RATKA)

PPPL#92X0334

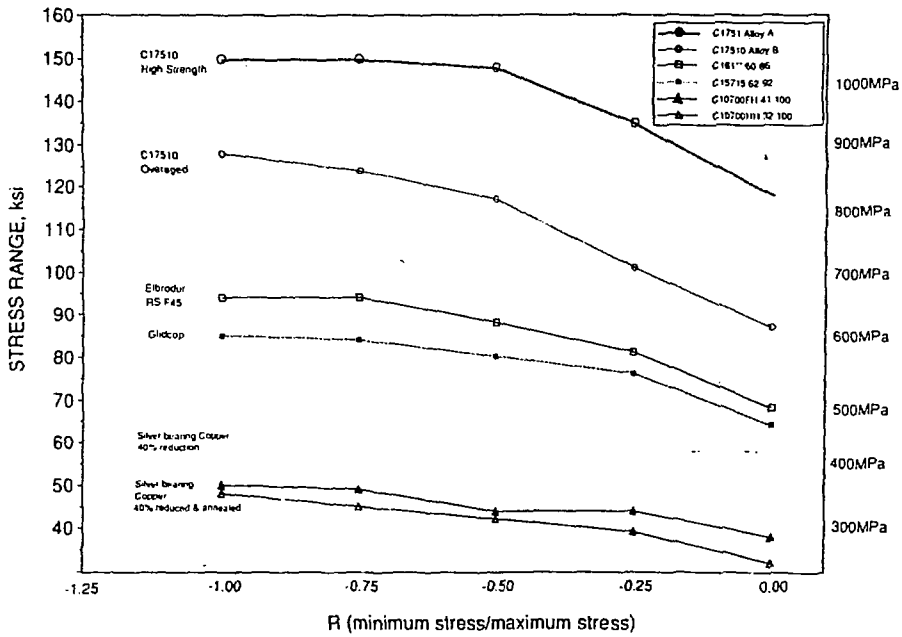

FIG. 2 (ZATZ, MURRAY, RATKA)

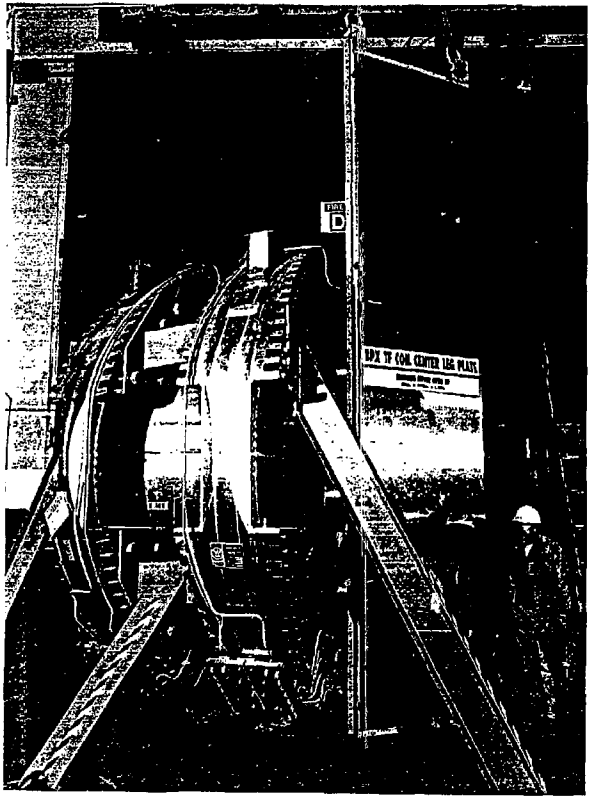

FIG. 3 (ZATZ, MURRAY, RATKA)

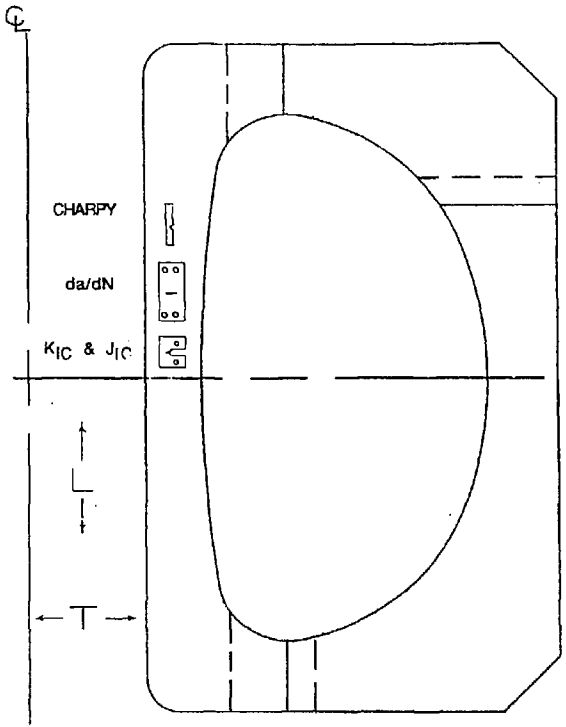

FIG. 5 (ZATZ, MURRAY, RATKA)

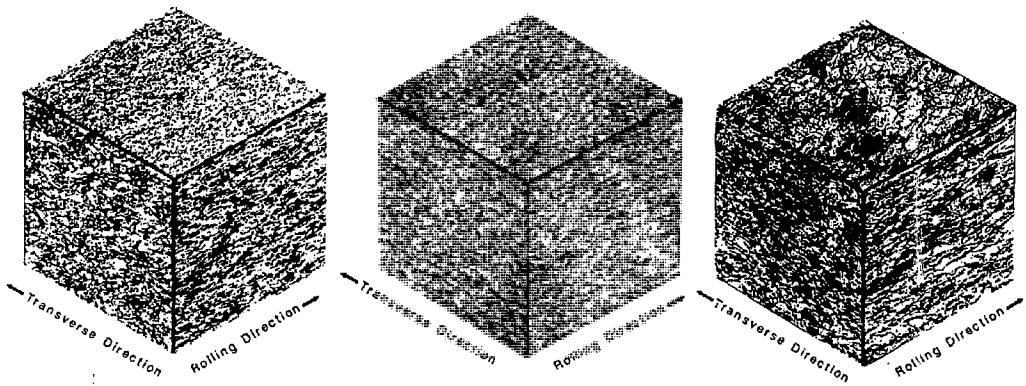

FIG. 4 (ZATZ, MURRAY, RATKA)

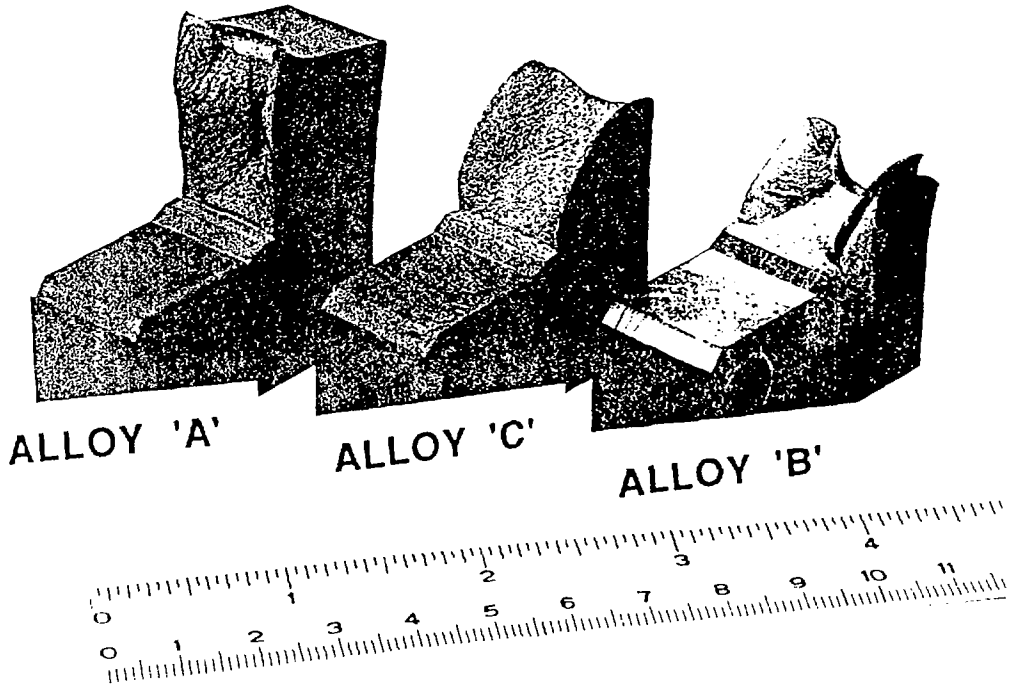

FIG. 6 (ZATZ, MURRAY, RATKA)

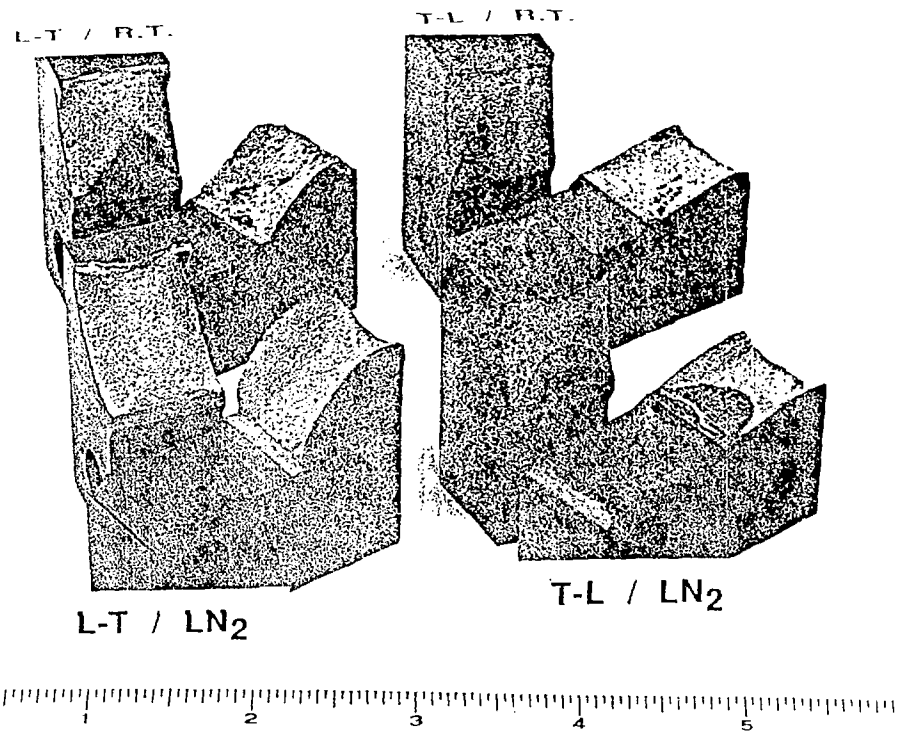

FIGURE 7 (ZATZ, MURRAY, RATKA)

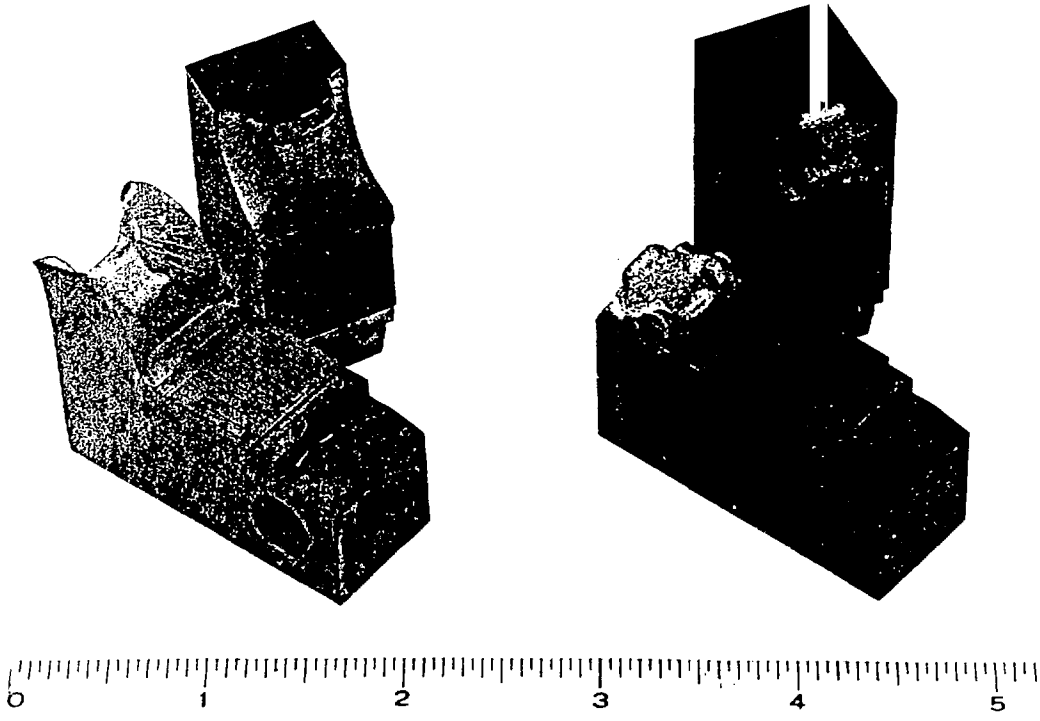

FIGURE 8 (ZATZ, MURRAY, RATKA)

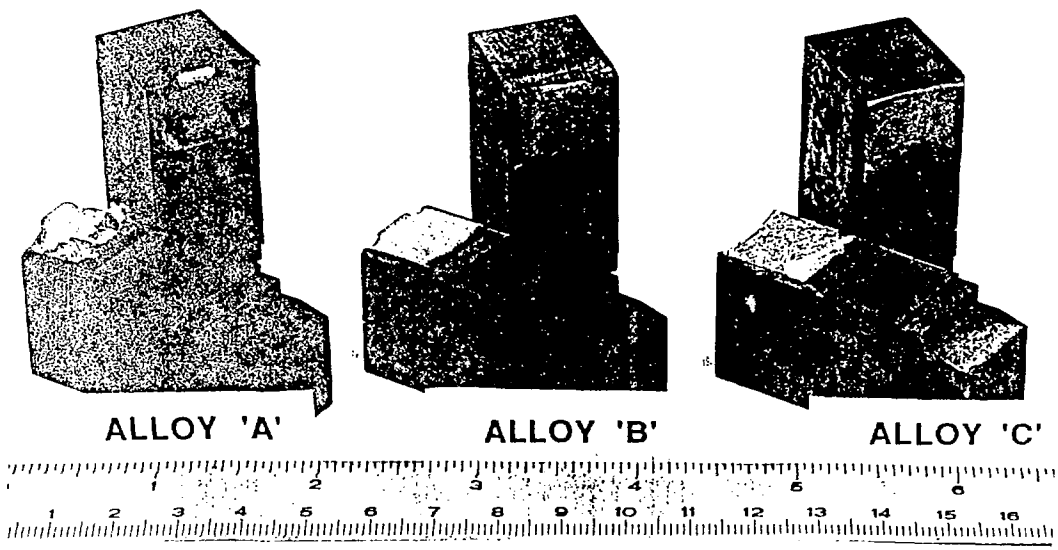

FIGURE 9 (ZATZ, MURRAY, RATKA)

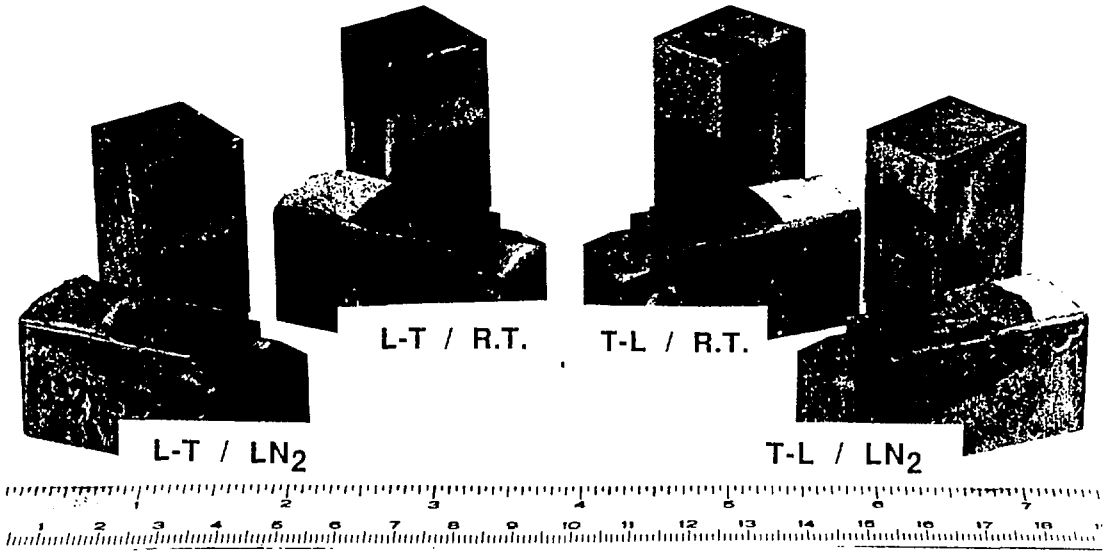

FIG. 10 (ZATZ, MURRAY, RATKA)

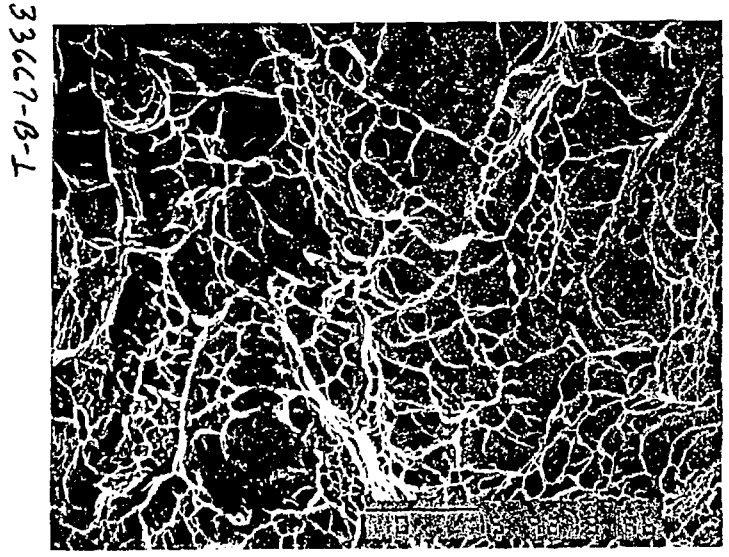

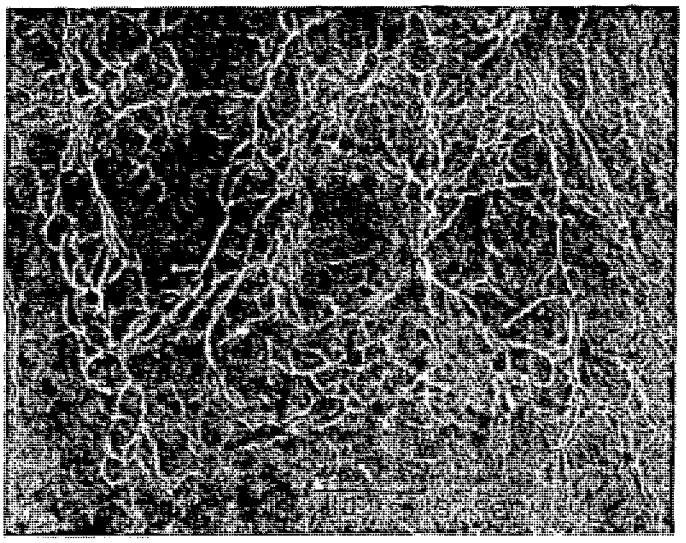

FIG. 11 TOP/BOTTOM (ZATZ, MURRAY, RATKA)

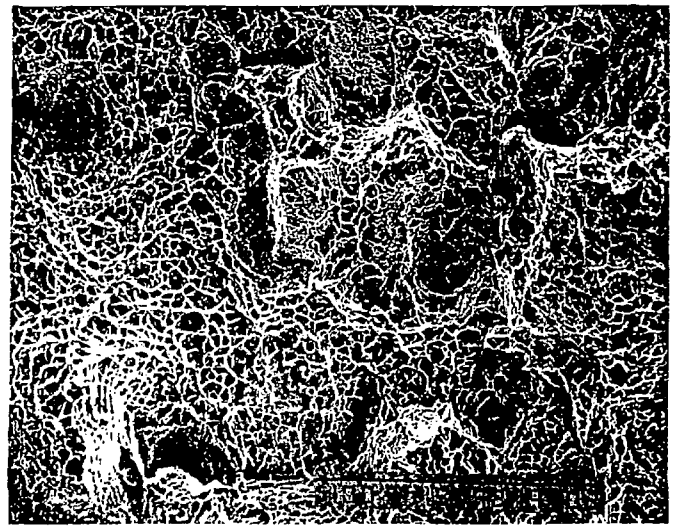

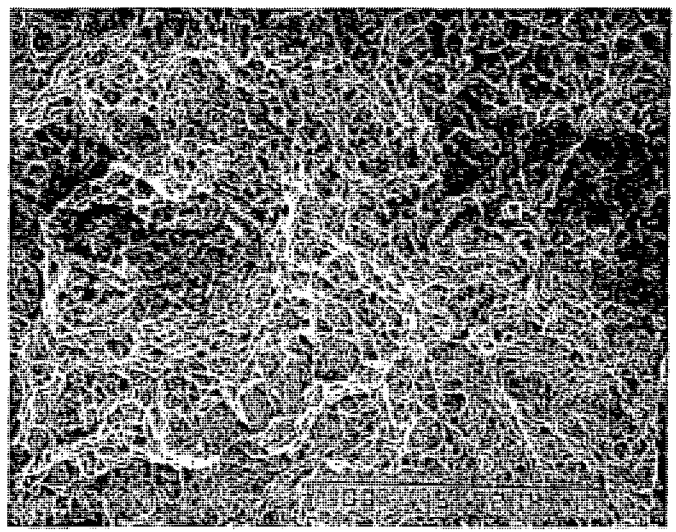

FIG. 12 TOP/BOTTOM (ZATZ, MURRAY, RATKA)

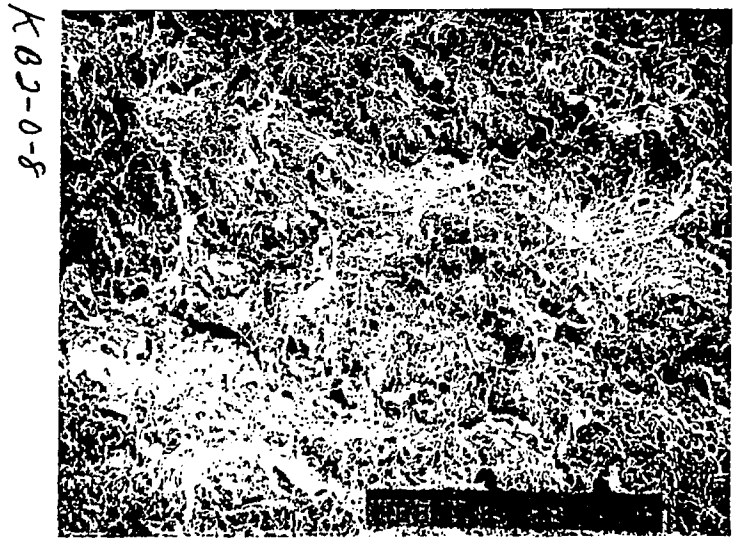

FIG. 13 (ZATZ, MURRAY, RATKA)

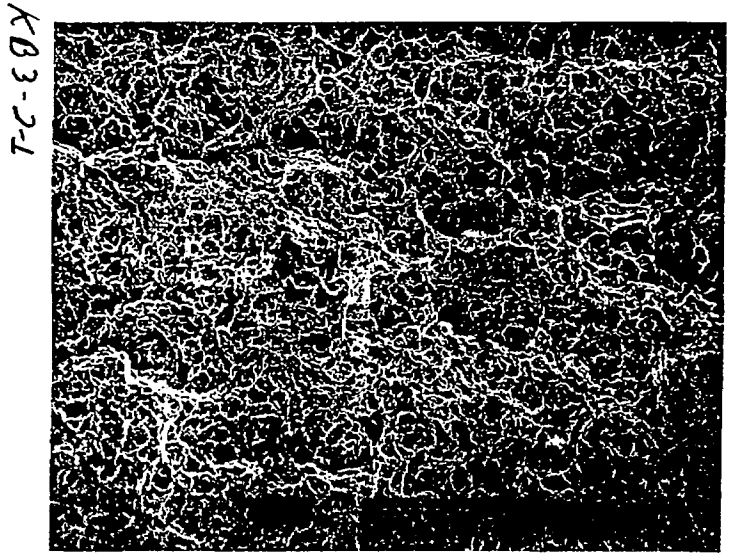

FIG. 14 (ZATZ, MURRAY, RATKA)

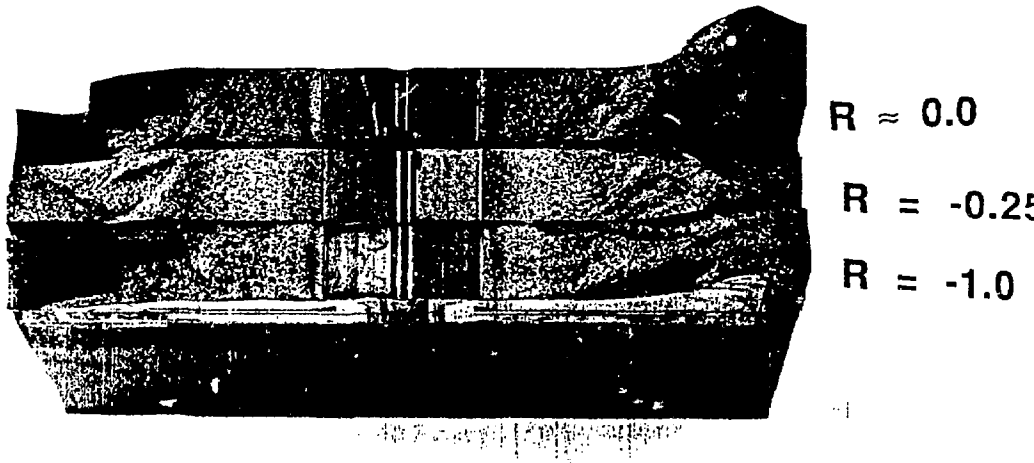

FIG. 15 (ZATZ, MURRAY, RATKA)

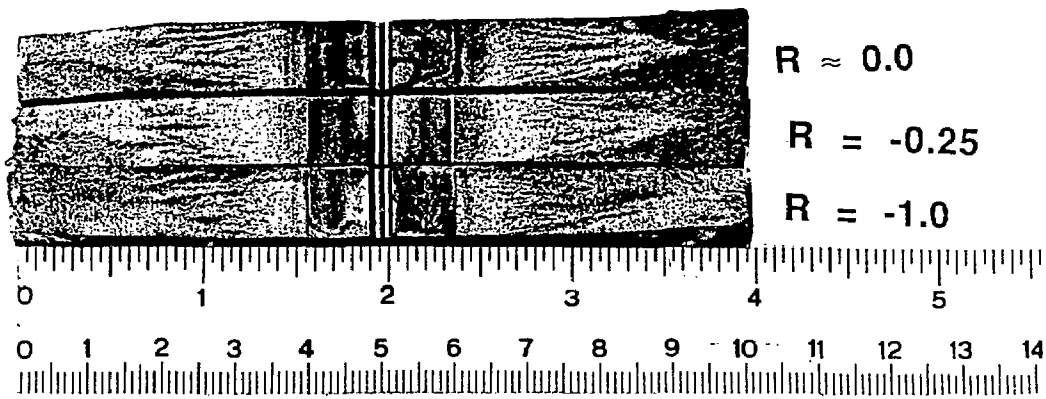

FIG. 16 (ZATZ, MURRAY, RATKA)

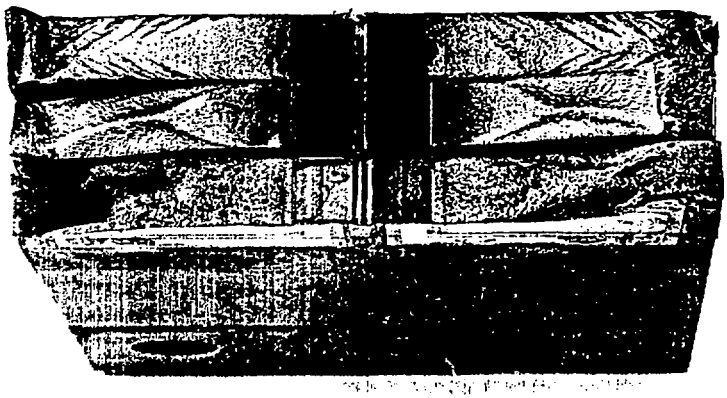

FIG. 17 (ZATZ, MURRAY, RATKA)

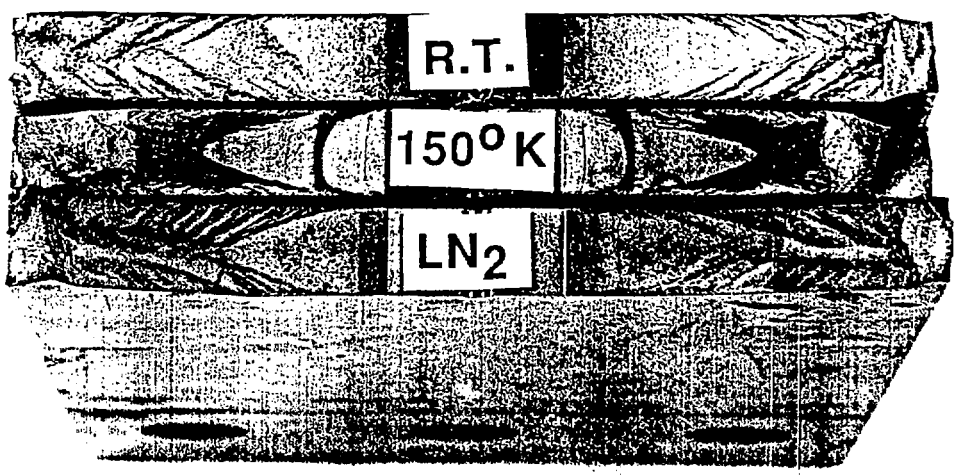

FIG. 18 (ZATZ, MURRAY, RATKA)

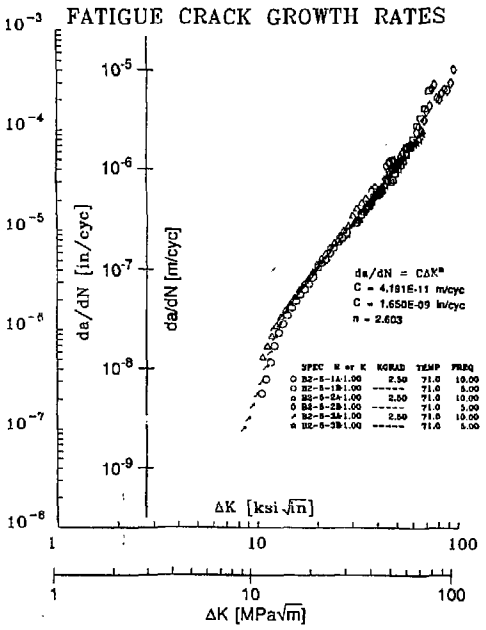

FIG. 19 (ZATZ, MURRAY, RATKA)

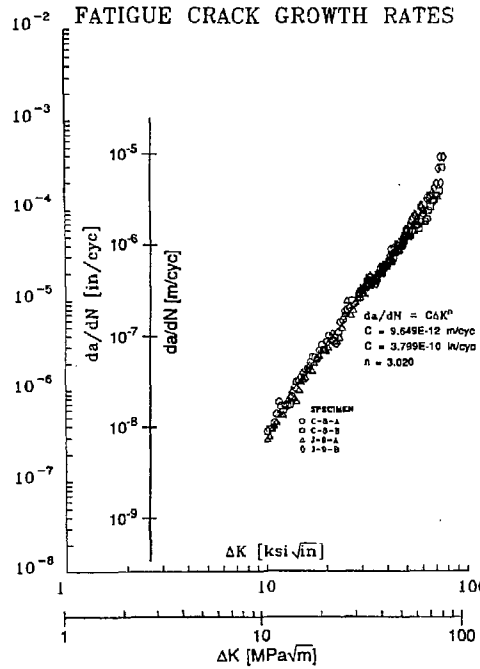

FIG. 20 (ZATZ, MURRAY, RATKA)